



Technical Report
FCRC-TR 97- 10

Determination of Interface Height From Measured Parameter Profile in Enclosure Fire Experiment

FCRC Project 4
Fire Safety System Design Solutions
Part A – Core Model & Residential Buildings

Fire Code Reform Research Program
November 1997

Important Notice

This Report has been prepared for work commissioned by Fire Code Reform Centre Limited and has been released for information only.

The statements and conclusions of the Report are those of the author(s) and do not necessarily reflect the views of Fire Code Reform Centre Limited , its Board of Directors or Members.

Neither the authors, Fire Code Reform Centre Limited, nor the organisations and individuals that have contributed, financially or otherwise, to production of this document warrant or make any representation whatsoever regarding its use.

Background

The Fire Code Reform Research Program is funded by voluntary contributions from regulatory authorities, research organisations and industry participants.

Project 4 of the Program involved development of a Fundamental Model, incorporating fire-engineering, risk-assessment methodology and study of human behaviour in order to predict the performance of building fire safety system designs in terms of Expected Risk to Life (ERL) and Fire Cost Expectation (FCE). Part 1 of the project relates to Residential Buildings as defined in Classes 2 to 4 of the Building Code of Australia.

This Report was relevant to the project activities in support of the Model's development and it is published in order to disseminate the information it contains more widely to the building fire safety community.

Acknowledgements

Since inception of the Fire Code Reform Research Program in 1994 the Australian Building Codes Board has been its principal financial contributor. Substantial funds have also been provided by Forest and Wood Products Research and Development Corporation and generous contributions have been received from a number of industrial and financial entities and individual donors.

The Board and management of Fire Code Reform Centre Ltd acknowledge with sincere thanks receipt of all these financial contributions. The company also acknowledges the kind permission of the author(s) and the Centre for Environmental Safety and Risk Engineering at Victoria University of Technology to re-produce and publish this document.

Comments

Comments on the content or other aspects of this document are always welcome and should be addressed to:- Fire Code Reform Centre Limited, Suite 1201, 66 King Street, Sydney, NSW 2000, Australia. Tel: No:- +61(2) 9262 4358 Fax No:- +61 (2) 9262 4255

Yaping He, Anthony Fernando and Mingchun Luo
 Centre for Environment Safety and Risk Engineering
 Victoria University of Technology, Melbourne, Australia.

ABSTRACT

Two methods are proposed in this paper for determining the smoke layer interface height from parameter profiles measured in enclosure fires. The schemes are based on mathematical considerations of uniformity and optimisation, and involve no subjectivity and empiricism. The application of these two methods to a set of experimental data revealed that the two methods gave close results of the interface height but different to that determined with the N-percentage rule. The dependence of the zone average of the measured quantities on the interface height is discussed. The predictions of a two-zone model is also included for comparison.

NOMENCLATURE

a, b, c	constants.	A	integration region
f, g	arbitrary functions.	ϕ	bi-valued function.
F, G	integrals of f and g .	σ	standard deviation.
H	height (m).	ξ	linearly transformed variable.
k	constant.		
m	constant.		
		<i>Subscript</i>	
N	value in the N-percentage rule.	av	average.
p	arbitrary parameter.	i	interface.
Q	heat release rate (MW).	ι	index.
R	real domain.	l	lower layer.
	integral ratio function.	r	room.
T	temperature (K, °C).	t	total.
x	variable.	u	upper layer.
Y	coordinate variable.		
z	variable.		

INTRODUCTION

Interface height is an important parameter in zonal approach to fire modelling and in fire safety calculations in general. Computer modelling, particularly the zone modelling approach to fire growth and smoke spread has undergone vast development in the past few decades^{1,2}. The zone concept in fire modelling evolved from the experimental observation of the stratifying effect associated with smoke movement in building enclosures³. Hot smoke generated in the fire plume tends to move along the upper part of the enclosures due to buoyancy effect and relatively cool air tends to remain at the lower part. There is typically a horizontal interface between the upper smoke layer and the lower clear air. Smoke density undergoes a rapid, though continuous, change across this interface region. In the zone model approach, an enclosure is often divided into two zones - the upper hot zone and the lower cool zone^{4,5}. Each zone is treated as a control volume and conditions in each control volume are assumed to be in equilibrium and uniform. While the total volume of the enclosure is fixed, the interface between the two zones may rise and fall as the result of emission and ventilation processes. The zone model approach was introduced to reduce computation complexity without unduly sacrificing accuracy.

The zone approach, on one hand, simplifies the numerical computation and gives quick estimates of physical conditions in building enclosures during fires, and on the other, brings challenges to experimenters to produce, from experimentally measured data, the appropriate and meaningful quantities for comparison with the zone model predictions. One of the challenges is the determination of the position of the zone interface. Under the two-zone assumptions, physical parameters are no longer continuously distributed over the elevation. Discontinuity occurs at the interface. However, the distributions of parameters in reality are not only continuous but, in many cases, may not experience “rapid” changes. The two-zone concept is a simplification of reality. Quite often, we want to draw a definite division of black and white out of a grey picture and round off blur into clear margins⁶. A profound discussion on the simplification of reality for modelling purpose is beyond the scope of this paper. The question relevant to the present work is how we perform the rounding off and draw a demarcation line between the hot smoke and relatively cool air in a fire enclosure.

A number of schemes for the determination of the interface height have been proposed in the literature, notably the N-percentage rule by Cooper *et al*⁷ and the upper zone averaging and mass equivalency technique by Quintiere *et al*⁸. Janssens and Tran⁹ developed another technique using a combination of the method by Quintiere *et al* and the maximum gradient method by Emmons¹⁰ (though the latter was originally proposed for determining the neutral plane position at a vertical vent). All of these methods admit of some degree of subjectivity and empiricism.

For example, when using the N-percentage rule to process experimentally measured temperature data, one is often baffled with the selection of the N value. A range of values (10, 15 and 20) have been suggested by Cooper *et al*⁷, and, as was admitted, these selections were quite subjective. If the temperature gradient around the interface region is reasonably large, then the selection of the N value for the N-percentage method is not so critical as is explained in Fig. 1(a). Even a value of $N=50$ would yield an interface height H_i that is very close to the interface height determined with the same method for $N=15$ or $N=20$. However, if the temperature is gradually increasing with elevation y , the interface height as determined with the N-percentage method will be very sensitive to the value of N as is explained in Fig. 1(b). Examples of gradual increasing temperature in the upper layer to the ceiling of an enclosure

are usually found in areas remote from the room of fire origin and in long corridors where counter flow mixing is strong^{11,12}.

Another drawback of the N-percentage rule is its inability to determine the interface height when gas in the lower region of an enclosure is warmed up so that temperature there is substantially greater than the ambient. The situation is explained in Fig. 2 where the temperature line of $T=T_{amb}$ fails to intersect with the temperature distribution profile.

In the development of the N-percentage rule, the interface height $H_i(t)$ was assumed to be a monotonic decreasing function in time'. The introduction of this assumption, though not fully clarified by the original authors, tends to limit the use of the method to the period from fire start to the time of minimum interface height.

Subjectivism also permeated into the techniques employed by Quintiere et al⁸ and Janssens and Tran⁹. Their approach to the estimation of the upper layer temperature are similar to that of the N-percentage rule. As Janssens and Tran pointed out that there is no justification of the approach, other than that it is convenient and seems to give reasonable results.

In the two-zone modelling approach, it is assumed that, except through plumes, there is no mass transferred across the interface between the two zones². However, in reality, the formation of a smoke layer in an enclosure involves complicated physical processes such as the buoyancy driven turbulence mixing and radiation heat transfer. A visually observed "interface" may not represent the boundary across which no mass is transferred. What is observed around the interface region is associated with convective and diffusive mixing. A rigorous definition of the interface based on physical considerations may be very difficult. Instead, the present study bases the definition on mathematical considerations.

DETERMINATION OF THE INTERFACE HEIGHT

The objective of the present study is to divide a measured parameter profile into two regions such that the averaged bi-valued distribution give; the closest representation of the original distribution. The basic idea rests on the analysis of the uniformity of parameter distributions in two divided regions.

Average Quantity and Uniformity

The interface determination scheme discussed in the present study is based on an analysis of average quantities over a given region. First, let two averaging schemes¹³ be introduced. In a typical enclosure fire, variations in parameters along the horizontal direction is usually negligible, and the parameters are expressed as functions of elevation y only. A direct average scheme for a parameter p is written as

$$P_{av1} = \frac{1}{(b-a)} \int_a^b p(y) dy . \quad (1)$$

Another is the reciprocal average scheme

$$p_{av2} = (b-a) \int_a^b \frac{1}{p(y)} dy . \quad (2)$$

It can be shown that the ratio of these two average quantities is not less than one for any distribution of p (see Appendix). To be more precise, if $p(y)$ is a real valued function which does not change sign over the region $[a, b]$, then the inequality

$$\frac{P_{av1}}{P_{av2}} \geq 1 \quad (3)$$

always holds. This ratio attains unity for any given finite region if p is uniformly distributed in that region. Denote the ratio of p_{av1} to p_{av2} as r and name it as the integral ratio. When the parameter distribution in a region deviates severely from the uniform condition, significant difference between p_{av1} and p_{av2} , and, therefore, large value of r , can be expected. The integral ratio r is in fact a measure of uniformity of parameter p in region $[a, b]$. The closer the r value is to unity, the more uniform is the p distribution over the given region.

Integral Ratio Method

We start with the analysis of the ratio r . Suppose that the parameter profile $p=p(y)$ is defined in the region $[0, H_r]$ and is divided by a line $y=H$, where H is greater than zero and less than H_r . Apply the two averaging schemes expressed by Eqs. (1) and (2) to the parameter distributions over two sub-regions $[0, H]$ and $[H, H_r]$ to obtain two ratios r_u and r_l

$$r_u = \frac{1}{(H_r - H)^2} \int_H^{H_r} p(y) dy \int_H^{H_r} \frac{1}{p(y)} dy, \quad (4)$$

$$r_l = \frac{1}{H^2} \int_0^H p(y) dy \int_0^H \frac{1}{p(y)} dy. \quad (5)$$

The subscripts u and l denote upper layer and lower layer respectively. Define a new quantity r_t as the sum of the two integral ratios, that is

$$r_t = r_u + r_l. \quad (6)$$

For a given parameter distribution $p(y)$ over the region $[0, H_r]$, the total integral ratio r_t is a function of H , i.e. $r_t = r_t(H)$ and has a minimum value within the region. The interface height H_i is defined as the value of H at which r_t attains the minimum

$$r_t(H_i) = \min(r_t). \quad (7)$$

The above described method does not rely on an external reference parameter, such as the ambient condition, nor on any other parameters of empirical nature. The only reference is the absolute zero of the parameter p itself and the only constraint for the method is that the parameter distribution must remain either positive or negative in the whole region of $[0, H_r]$.

Least Square Method

Discussed in this subsection is a method that removes all references and constraints. The data reduction process of finding an interface and obtaining zone average quantities can be regarded as a curve fitting process. In this process, we want to represent a measured continuous curve by this bi-valued function (Fig. 3)

$$\phi(y, H) = \begin{cases} p_l = \text{constant}, & \text{for } y < H; \\ p_u = \text{constant}, & \text{for } y > H, \end{cases} \quad (8)$$

where the two constant values p_l and p_u are averages of $p(y)$ in the lower and upper regions $[0, H]$ and $[H, H_r]$ respectively

$$p_l = \frac{1}{H} \int_0^H p(y) dy, \quad (9)$$

$$p_u = \frac{1}{H_r - H} \int_H^{H_r} p(y) dy.$$

For a given parameter profile $p(y)$, the average values p_l and p_u are functions of H .

The deviation of $p(y)$ from $\phi(y, H)$ are estimated as

$$\sigma^2 = \frac{1}{H} \int_0^H [p(y) - p_l]^2 dy + \frac{1}{H_r - H} \int_H^{H_r} [p(y) - p_u]^2 dy. \quad (10)$$

For a given distribution $p(y)$, Eq.(10) is a function of H , and has a minimum value in the region bounded by zero and H_r . The interface height H_i is defined as the value of H such that at which the deviation expressed by Eq.(10) attains the minimum, that is

$$\sigma^2(H_i) = \min[\sigma^2(H)]. \quad (11)$$

Since the deviation is calculated from the difference between $p(y)$ and its means in $[0, H]$ and $[H, H_r]$, the absolute value of p is irrelevant. Adding any arbitrary constant to the distribution $p(y)$ will not alter the evaluation of σ^2 and hence H_i . Therefore, unlike the N-percentage rule, the least square method will always yield a definite value of interface height. However, a definite value of H_i does not always mean that a clearly defined interface and two distinctive zones exist. For example, even if the variation in parameter p is very small over the entire region $(0, H_r]$, the least square method will still work out a value of H_i between 0 and H_r , plus two very close average values of p for the two zones separated by line $y = H_i$. It is easy to discern that the entire region can be treated as a single zone. Hence, the meaning of interface height H_i must be interpreted in conjunction with the two average zone values of parameter p .

The two methods discussed above have been implemented in a computer data processing program. For a given discrete parameter profile, the program uses the golden search method¹⁴ to minimise the total integral ratio r_t (Eq.(6)) and the deviation σ^2 (Eq.(10)) and to obtain the corresponding interface heights. In calculating the integral terms in Eqs. (9) and (10), the parameter is assumed to have a linear distribution between any two adjacent measurement points. The numerical integration procedure is the same as that described in Ref. 13 in detail.

APPLICATION

In this section, examples are given to demonstrate the application of two proposed methods to experimentally measured temperature profiles. Comparisons are made between the two methods and the N-percentage rule.

The Experiment

The experiments were carried out in the Experimental Building-Fire Facility at Victoria University of Technology, Australia. The facility is a full-scale prototype building which has four stories connected by a lift shaft, a stairwell and air handling shafts. A detailed description of the facility can be found in Ref. 12. Fig. 4 schematically depicts the layout of the first floor on which the fire source was located. The bum room on Level 1 had a

dimension of 5.4m×3.6m×2.4m high. The instrumentation for the experiments are described below.

A weighing system was established to record the mass of fuel on two floor the experiments. The mass release rate was deduced from the derivative of the record against time. A thermocouple array (marked as TC6 in Fig. 4) was vertically placed at the centre point between the bum room door, D1, and the stairwell door, D9 in the first floor corridor which was 15.6 m long, 1.4 m wide and 2.57 m high. The array consisted of 9 thermocouples with a spacing of 250 mm between any two adjacent thermocouples. The lowest thermocouple was 250 mm above the floor. Thermocouples were also placed in many other locations in the building. However, only the temperatures measured with array TC6 in the corridor were analysed for the purpose of verification of the interface determination techniques developed in this study. The locations of the instruments on a horizontal level are illustrated in Fig. 4.

A series of fire experiments has been conducted. The results presented in this paper are the two cases where the arrangements were for flashover fires. Case 1 is associated with the air-handling system off; and Case 2 with the air-handling system on. When the air-handling system was turned on, the smoke management operation of the air-handling system was controlled by a smoke detector which was placed in a duct (see Fig. 4) at the ceiling level. The air-handling system was operating at the start of the fire experiment. Two air supply ducts (0.4m×0.4m) were located on the ceiling. The air flow rates of these two inlets were 46 and 50 l/s respectively. The system switched to smoke management mode automatically at about 80 seconds when the smoke detector operated; about 800 l/s of air (smoke) was then extracted from the bum room. The doors D1 and D9 were open during the experiments. The stair doors to other levels also remained open. All other doors in the building were closed. All the doors in the building had a dimension of 0.8m×2.0m high.

The fuel configuration in the bum room for these two experiments is illustrated in Fig. 4. The fuel load included a three-seat couch, two single-seat sofa, two coffee tables, and two book shelves with phone books. The couch and one coffee table were located on the small platform, the others were on the large platform. The total fuel load is 542.1 kg for Case 1 and 539.7 kg for Case 2, corresponding to two fuel load densities of 27.9 kg/m² and 27.8 kg/m² of floor area respectively.

Data Analysis

Two N value (15 and 20) were selected in this study for the N-percentage rule. Although this rule is limited to fires of ever descending smoke layer⁷, the present study extended its application to the situations where recession of smoke layer did occur.

Before various methods were applied to the measured temperature profile to determine the interface height, the profile at a given time was linearly extrapolated down to the floor and up to the ceiling of the corridor. The error introduced by this extrapolation was believed to be small. Once an interface height H_i is determined, the average temperatures for the upper and lower zones are calculated from¹³

$$T_u = (H_t - H_i) \int_{H_i}^{H_t} \frac{1}{T} dy, \quad (12)$$

and

$$T_l = H_i \int_0^{H_i} \frac{1}{T} dy. \quad (13)$$

The absolute temperature is used in the analysis.

Result and Discussion

Figure 5 shows the measured results of heat release rate and a surface plot of the measured temperature profile in the middle of the first floor corridor as a function of time for Case 1. Layering effect can be discerned- from the temperature changes along the vertical direction at given times. However, the temperature distribution does not indicate a distinct interface between the hot upper layer and the relatively cool lower layer. Temperature continuously increased with height y up to the region near the ceiling of the corridor. Around 395 seconds after the ignition, the glass window in the bum room was broken. The heat release rate reached the maximum at about 900 and started to decay after that. However, the peak temperature in the corridor lagged behind the maximum heat release rate measured in the bum room by about 250 seconds.

Presented in Fig. 6 are the interface heights determined from the temperature profiles (as shown in Fig. 5) measured in the corridor in the Case 1 experiment. The results of the N -percentage rule (for $N=20$ and $N=15$), the integral ratio method and the least square method are compared in this figure. It is seen that the interface heights determined with the latter two methods are close to each other, whereas, those determined with the N -percentage rule are substantially lower. Different N values resulted in somewhat different interface heights for the temperature profiles obtained in this experiment. It is also seen that the N -percentage rule failed to detect the recession of the smoke layer during the decay period of the fire (see heat release rate and temperature profiles in Fig. 5). The integral ratio method produced somehow more stable result than the least square method. The latter appeared to be sensitive to some disturbance in the temperature distribution.

The average zone temperatures in an enclosure are coupled with the position of zone interface, since the latter determines the sizes of each zone. For a given temperature profile, the zone temperatures are functions of the interface height. For a temperature profile monotonically increasing with elevation y , the higher the interface is, the greater are both the upper and lower zone temperatures. The zone average temperatures corresponding to various interface heights as given in Fig. 6 are presented in Figs. 7 and 8.

It is not intended in the present work to validate any computer model. Nevertheless, the predictions of a two-zone model called CFAST⁴ are included in Figs. 6, 7 and 8 for comparison. The measured heat release rate as shown in Fig. 5(a) was used as the input data to the model. Figure 6 reveals that the CFAST model predicted an earlier descending of the smoke layer than that determined from the measured temperature profile in the corridor. In a multi-room fire, the initial flow regime is attributed to the thermal expansion and smoke filling processes in the room of fire origin⁹. This initial flow, though has no significant temperature rise and does not alter the temperature distribution in the adjacent room, is regarded by the zone model as smoke injection to the adjacent room. Under the assumptions of the zone model, smoke travels from one end of an enclosure to the other at an infinite speed and an upper layer is formed as soon as there is gas movement. As a result, the CFAST model predicts an immediate formation of "smoke layer" in the adjacent room as soon as the fire is ignited in the room of fire origin. In reality, smoke propagates along a corridor in the form of gravity-current¹⁵, or ceiling jet¹⁶. The smoke front which establish itself as a hydraulic jump travels at a finite velocity. Therefore, for the experiments conducted in this study, a time delay was observed between the ignition of the fire in the bum room and the detection of the smoke

front at the centre of the first floor corridor, some distance downstream of the bum room door (Fig.4).

The measured results from Case 2 experiment are presented in Fig. 9. Both the heat release rate in the bum room and the temperature measurement in the corridor indicate that flashover stage was not reached during this experiment because of the removal of the product heat by the extraction of smoke. The bum room window remain intact. Figures 10, 11 and 12 display the interface heights, the average upper zone and lower zone temperatures as obtained from the measured experimental data. The traces of the interface height determined with the integral ratio and the least square methods are very closed to each other in this case. As a consequence, the average zone temperatures according to these interface heights are indistinguishable from each other (see Figs. 11 and 12). Surprisingly, the N-percentage rule did work out the receding smoke layer height during the decay period of this experiment. Again, the interface heights by this rule for $N=15$ and $N=20$ are lower than those by the other two methods. The agreement between the predicted results of CFAST and the measured results is poor for this experiment.

CONCLUSION AND FURTHER DISCUSSION

Attempt has been made in **this** study to eliminate subjectivity and empiricism from some of the data processing procedure in experimental fire research. The two methods discussed herein for determining the interface height from the measured parameter distributions are based on the minimisation of certain characteristic parameters. These methods correlate the interface height to the entire distribution of the measured physical quantities rather than to some isolated measurement points. The application of the two methods to a set of experimental data revealed that the two methods gave close results of interface height but different from that determined with the N-percentage rule for the same temperature profile. The advantage of the least square method over integral ratio method is that the former does not depend on the absolute value of the measured quantity. However, it appears to be more sensitive to spatial fluctuations of the temperature profile.

For a given parameter profile, the zone average quantities depend on the position of the interface. Different values of the interface height as determined with different methods for the same distribution profile may result in significant differences in the zone average quantity. It appears from the present study that the newly proposed methods tend to yield higher values of the interface height and the average zone temperatures in an enclosure next to the bum room than that obtained with the N-percentage rule. From risk assessment view point, the over-estimate of average zone conditions (temperature, smoke density and toxic species concentrations) are more desirable since it would lead to more conservative judgement in fire safety analysis¹⁷.

The concept of zone modelling approach was drawn from experimental observation of smoke density in enclosure fires. The distribution of smoke density is governed by mass transfer via two mechanisms – convection and diffusion. Temperature distribution, on the other hand, is governed by heat transfer via three mechanisms – convection, conduction and radiation. Therefore, the two distributions do not in general coincide, or are not similar to each other. The correlation between the interface height as determined from temperature distribution and that as determined from smoke density and visibility distribution has not been fully discussed in the literature. The question remain unanswered whether the visually observed interface does correspond to the interface across which no mass transfer occurs. Verifications of the integral ratio method and the least square method with the parameter of smoke density, or visibility are

needed. Experiments are being designed at the Centre for Environmental Safety and Risk Engineering to carry out such investigation.

ACKNOWLEDGEMENT

This work was conducted under the support of an Australian Research Council Collaborative Research Grant in conjunction with BHP and National Association of Forest Industry. The experimental work was part of a research project which is coordinated by Prof. Vaughan Beck and supported by Fire Code Reform Centre Ltd.

REFERENCES

- 1 Friedman, R., 1992, "An International Survey of Computer Models for Fire and Smoke," *J. Fire Prot.* pp.% I-92.
- 2 Quintiere, J. G., 1995, "Compartment Fire Modeling," in *The SFPE Handbook of Fire Protection Engineering*, 2nd edition, DiNenno, P. J., ed., Society of Fire Protection Engineers, Boston. pp.3.1253.133.
- 3 Kawagoe, K., *Fire Behaviour in Rooms. Building Fire Research Institute*, Ministry of Construction (Japan), Report No. 27, Tokyo, 1958.
- 4 Peacock, R. D., G. P. Forney, P. Reneke, R. Portier and W. W. Jones, 1993, "CFAST, the Consolidated Model of Fire Growth and Smoke Transport," NIST Technical Note 1299, Building and Fire Research Laboratory, National Institute of Standards and Technology, Gaithersburg, MD 20899-0001, USA.
- 5 Brani, D. M. and W. Z. Black, 1992, "Two-Zone Model for a Single-Room Fire," *Fire Safety J.*, 19, pp.189-216.
- 6 Kosko, B., 1993, *Fuzzy Thinking - The New Science of Fuzzy Logic*, Flamingo, London, p.21.
- 7 Cooper, L. Y., Harkleroad, M., Quintiere, J. and Rinkinen, W., 1982, "An Experimental Study of Upper Hot Layer Stratification in Full-Scale Multi-Room Fire Scenarios", *Journal of Heat Transfer*, Vol. 104, November, pp.741-749.
- 8 Quintiere, J. G., K. Steckler and D. Corley, 1984, "An Assessment of Fire Induced Flows in Compartments", *Fire Science and Technology*, 4(1), pp. I-14.
- 9 Janssens, M. L. and Tran, H. C., 1992, "Data Reduction of Room Tests for Zone Model Validation", *Journal of Fire Sciences*, 10, November/December 1992, pp.528-555.
- 10 Emmons, H. W., 1995, "Vent Flows," in *The SFPE Handbook of Fire Protection Engineering*, 2nd edition, DiNenno, P. J., ed., Society of Fire Protection Engineers, Boston. pp.2.40-2.49.
- 11 Peacock, R. D., W. W. Jones and R. W. Bukowski, 1993, "Verification of a Model of Fire and Smoke Transport," *Fire Safety J.*, 21, pp.89-129.
- 12 He, Y., and V. Beck, 1996, "Smoke Spread Experiment in a Multi-Storey Building and Computer Modelling", *Fire Safety Journal.*, 28(2), pp. 139-164.
- 13 He, Y., 1997, "On Experimental Data Reduction for Zone Model Validation," *Journal of Fire Sciences*, 15(2), pp 144- 161.

- 14 Press, W. H., Teukolsky, S. A., Vetterling, W. T. and Flannery, B. P., 1992, *Numerical Recipes – The Art of Scientific Computation*, 2nd ed., Cambridge University Press.
- 15 Rehm, R. G., Cassel, K. W., McGrattan, K. B. and Baum, H. R., “Gravity-Current Transport in Building Fires”, *Transport Phenomena in Combustion - Proceedings of the Eighth International Symposium on Transport Phenomena in Combustion*, Ed. Chan, S. H., pp. 745-756.
- 16 Evans , D. D, 1995, “Ceiling Jet Flows”, *The SFPE Handbook of Fire Protection Engineering*, 2nd edition, the National Fire Protection Association, Ed. DiNenno, P. J. et al, pp.2.33-2.39.
- 17 Beck, V. R., 1991, “Fire Safety System Design Using Risk Assessment Models: Developments in Australia,” *Fire Safety Science- - Proceedings of the Third International Symposium*, the University of Edinburgh, Scotland, pp.45-59.

APPENDIX

Let f be a real, non-zero valued and integrable function of x in the region $[a, b]$ of real domain R and g the reciprocal of f . We have

$$fg = 1 \tag{A.1}$$

The assertion expressed in Eq.(3) is equivalent to

$$\frac{1}{\Delta^2} \int_{\Delta} f dx \int_{\Delta} g dx \geq 1, \tag{A.2}$$

where A is the region of integration.

We take two steps to prove the inequality as expressed by Eq.(A.2). Firstly, we make the approximation that the function is piecewise linear, and prove that this inequality holds for each linear interval. Then, we prove that it holds for a union of multiple intervals in which it holds individually.

Now, we wish to show that for an arbitrary linear function $f(x)=mx+c$, where m and c are constants,

$$\frac{1}{\Delta^2} \int_a^{a+\Delta} \frac{dx}{mx+c} \cdot \int_a^{a+\Delta} (mx+c) dx \geq 1, m \neq 0, x \in R. \tag{A.3}$$

The function $g(x)=1/(mx+c)$ has a singularity if $f(x)=mx+c=0$ on the interval $[a, a+\Delta]$. Thus, $f(x)$ must be strictly negative or strictly positive on this interval. When it is strictly negative, both integrals will be negative, and the resulting product will be positive. Thus, we need only consider the case $mx+c > 0, \forall x \in [a, a+\Delta]$. Without loss of generality, we introduce a linear transformation $\xi=x-a$ such that the integral terms in Eq.(A.3) become

$$\int_0^{\Delta} \frac{d\xi}{m\xi+k} = \frac{1}{m} \log(m\xi+k) \Big|_0^{\Delta} = \frac{1}{m} \log\left(1 + \frac{m\Delta}{k}\right) \tag{A.4}$$

and

$$\int_0^{\Delta} (m\xi + k) d\xi = \frac{1}{2} m\xi^2 + k\xi \Big|_0^{\Delta} = \Delta \left(\frac{m\Delta}{2} + k \right). \quad (\text{A.5})$$

where $k=ma+c$. Now the right hand side of Eq.(A.3) is equivalent to

$$\frac{1}{\Delta^2} \int_0^{\Delta} \frac{d\xi}{m\xi + k} \cdot \int_0^{\Delta} (m\xi + k) d\xi = \left(\frac{k}{m\Delta} + \frac{1}{2} \right) \log \left(1 + \frac{m\Delta}{k} \right). \quad (\text{A.6})$$

For simplification, let $z=m\Delta/k$ and r denote the above function, that is

$$r(z) = \left(\frac{1}{z} + \frac{1}{2} \right) \log(1+z). \quad (\text{A.7})$$

The mathematical constraint of this function is $z > -1$. Figure 13 is the plot of the function. This function is undefined at $z=0$, but the limit exists and is given by

$$\lim_{z \rightarrow 0} r(z) = 1. \quad (\text{A-8})$$

In the limiting case of $z=0$, we have either $m=0$ or $\Delta=0$. These two conditions correspond to the case where the linear function is the constant function $x=k$ (i.e. $m=0$), or the limit as the interval length approaches zero ($\Delta=0$).

To prove that $r=1$ at $z=0$ is the minimum of the function $r(z)$, it suffices to show that the first derivative of $r(z)$ is zero at $z=0$. When z approach zero, the first derivative of $r(z)$ is

$$\begin{aligned} \lim_{z \rightarrow 0} r'(z) &= \lim_{z \rightarrow 0} \left[\left(\frac{1}{z} + \frac{1}{2} \right) \cdot \frac{z+1}{z^2} - \frac{z^2}{z^2} \log(z+1) \right] = \lim_{z \rightarrow 0} \left[\frac{1}{z} + \frac{1}{2} - \log(z+1) \right] \\ &= \frac{1}{2} + \lim_{z \rightarrow 0} \left[\frac{z - (z+1) \log(z+1)}{(z+1)z^2} \right] = \frac{1}{2} + \lim_{z \rightarrow 0} \left\{ \frac{-1}{[2(z+1) + 4z](z+1)} \right\} = \frac{1}{2} - \frac{1}{2} = 0 \end{aligned}$$

Therefore, the function $r(z)$ has a minimum at $z=0$ and is never less than unity in the region $(-1, \infty)$. Note that the l'Hôpital's rule has been applied in the above derivation.

Next, we prove that the inequality Eq.(A.3) also holds for the sum of multiple intervals. The assertion is restated as follows.

Let Δ_i ($i=1, 2, \dots, n$) denote joint sub-regions in the x domain $[a, b]$. Let A be the union of Δ_i

$$\Delta = \sum_{i=1}^n \Delta_i \quad (\text{A-9})$$

Suppose that the inequality

$$\int_{\Delta_i} f dx \int_{\Delta_i} g dx \geq \Delta_i^2 \quad (i=1, 2, \dots, n) \quad (\text{A.10})$$

holds for each of the sub-region of A , then the inequality

$$\int_{\Delta} f dx \int_{\Delta} g dx \geq \Delta^2 \quad (\text{A.11})$$

also holds

Proof:

Let us consider a special case where $n=2$. Let F and G denote the integrations of f and g respectively in the region A . Let F_i and G_i denote the integrations of f and g in the sub-region A_i , ($i=1,2$). Then

$$F = \int_{\Delta} f dx = \int_{\Delta_1} f dx + \int_{\Delta_2} f dx = F_1 + F_2 \quad (\text{A.12})$$

and

$$FG = (F_1 + F_2)(G_1 + G_2) = F_1G_1 + F_1G_2 + F_2G_1 + F_2G_2 \quad (\text{A.13})$$

From the intermediate value theorem, there exists a value \bar{f}_1 such that

$$F_1 = \Delta_1 \bar{f}_1 \quad (\text{A.14})$$

\bar{f}_1 is often regarded as the mean value of f over the region Δ_1 . Similar expressions can be written for F_2 , G_1 and G_2

$$F_2 = \int_{\Delta_2} f dx = \Delta_2 \bar{f}_2, \quad G_1 = \int_{\Delta_1} g dx = \Delta_1 \bar{g}_1 \quad \text{and} \quad G_2 = \int_{\Delta_2} g dx = \Delta_2 \bar{g}_2 \quad (\text{A.15})$$

According to Eq.(A. 10)

$$F_1G_1 = \Delta_1^2 \bar{f}_1 \bar{g}_1 \geq \Delta_1^2, \quad (\text{A.16})$$

or

$$\bar{f}_1 \bar{g}_1 \geq 1. \quad (\text{A.17})$$

Similarly, we have

$$\bar{f}_2 \bar{g}_2 \geq 1. \quad (\text{A.18})$$

Now rewrite Eq.(A. 13)

$$\begin{aligned} FG &= \Delta_1^2 \bar{f}_1 \bar{g}_1 + \Delta_1 \Delta_2 \bar{f}_1 \bar{g}_2 + \Delta_1 \Delta_2 \bar{f}_2 \bar{g}_1 + \Delta_2^2 \bar{f}_2 \bar{g}_2 \\ &= \Delta_1^2 \bar{f}_1 \bar{g}_1 + \Delta_1 \Delta_2 (\bar{f}_1 \bar{g}_2 + \bar{f}_2 \bar{g}_1) + \Delta_2^2 \bar{f}_2 \bar{g}_2 \end{aligned} \quad (\text{A.19})$$

From Eqs.(A. 17) and (A.18)

$$\bar{f}_1 \bar{g}_2 + \bar{f}_2 \bar{g}_1 = \frac{\bar{f}_1}{\bar{f}_2} \bar{f}_2 \bar{g}_2 + \frac{\bar{f}_2}{\bar{f}_1} \bar{f}_1 \bar{g}_1 \geq \frac{\bar{f}_1}{\bar{f}_2} + \frac{\bar{f}_2}{\bar{f}_1} = \frac{\bar{f}_1^2 + \bar{f}_2^2}{\bar{f}_1 \bar{f}_2} \geq 2 \quad (\text{A.20})$$

Substituting the inequalities of Eqs.(A. 17), (A. 18) and (A.20) into Eq.(A. 19) yields

$$FG \geq \Delta_1^2 = \Delta^2 \quad (\text{A.21})$$

Now the inequality expressed by Eq. (A.1) with Eq. (A.9) for $n=2$ has been proved. The prove of the inequality for $n=3$ and hence any finite value, or even infinite number of divisions of A is straight forward, by using induction method.

List of Figures

- Figure 1.** Differences in the interface heights determined with various N values.
- Figure 2.** A case of indefinite interface according to the N-percentage rule.
- Figure 3.** Parameter distribution and the $\phi(y, H)$ function.
- Figure 4.** The first floor layout of the experimental facility and the fuel configuration in the bum room.
- Figure 5.** Measured results of the first experiment.
- Figure 6.** Interface heights determined with various methods for experiment 1
- Figure 7.** Average upper zone temperatures corresponding to various interface heights for experiment 1.
- Figure 8.** Average lower zone temperatures corresponding to various interface heights for experiment 1.
- Figure 9.** Measured results of the second experiment.
- Figure 10.** Interface heights determined with various methods for experiment 2
- Figure 11.** Average upper zone temperatures corresponding to various interface heights for experiment 1.
- Figure 12.** Average lower zone temperatures corresponding to various interface heights for experiment 2.
- Figure 13.** The graph of function $r(z)=(1/2 + 1/z) \log(z+1)$.

¹ Friedman, R., 1992, "An International Survey of Computer Models for Fire and Smoke," *J. Fire* 4(3), pp.81-92.

² Quintiere, J. G., 1995, "Compartment Fire Modeling," in *The SFPE Handbook of Fire Protection Engineering*, 2nd edition, DiNenno, P. J., ed., Society of Fire Protection Engineers, Boston. pp.3.1253.133.

³ Kawagoe, K., *Fire Behaviour in Rooms. Building Fire Research Institute*, Ministry of Construction (Japan), Report No. 27, Tokyo, 1958.

⁴ Peacock, R. D., G. P. Fomey, P. Reneke, R. Portier and W. W. Jones, 1993, "CFAST, the Consolidated Model of Fire Growth and Smoke Transport," NIST Technical Note 1299, Building and Fire Research Laboratory, National Institute of Standards and Technology, Gaithersburg, MD 20899-0001, USA.

⁵ Brani, D. M. and W. Z. Black, 1992, "Two-Zone Model for a Single-Room Fire," *Fire Safety J.*, 19, pp.189-216.

-
- ⁶ Kosko, B., 1993, *Fuzzy Thinking - The New Science of Fuzzy Logic*, Flamingo, London, p.21.
- ⁷ Cooper, L. Y., Harkleroad, M., Quintiere, J. and Rinkinen, W., 1982, "An Experimental Study of Upper Hot Layer Stratification in Full-Scale Multi-Room Fire Scenarios", *Journal of Heat Transfer*, Vol. 104, November, pp.741-749.
- ⁸ Quintiere, J. G., K. Steckler and D. Corley, 1984, "An Assessment of Fire Induced Flows in Compartments", *Fire Science and Technology*, 4(1), pp. 1- 14.
- ⁹ Janssens, M. L. and Tran, H. C., 1992, "Data Reduction of Room Tests for Zone Model Validation", *Journal of Fire Sciences*, 10, November/December 1992, pp.528-555.
- ¹⁰ Emmons, H. W., 1995, "Vent Flows," in *The SFPE Handbook of Fire Protection Engineering*, 2nd edition, DiNenno, P. J., ed., Society of Fire Protection Engineers, Boston. pp.2.40-2.49.
- ¹¹ Peacock, R. D., W. W. Jones and R. W. Bukowski, 1993, "Verification of a Model of Fire and Smoke Transport," *Fire Safety J.*, 21, pp.89-129.
- ¹² He, Y., and V. Beck, 1996, "Smoke Spread Experiment in a Multi-Storey Building and Computer Modelling", *Fire Safety Journal.*, 28(2), pp.139-164.
- ¹³ He, Y., 1997, "On Experimental Data Reduction for Zone Model Validation," *Journal of Fire Sciences*,
- ¹⁴ Press, W. H., Teukolsky, S. A., Vetterling, W. T. and Flannery, B. P., 1992, *Numerical Recipes – The Art of Scientific Computation*, 2nd ed., Cambridge University Press.
- ¹⁵ Rehm, R. G., Cassel, K. W., McGrattan, K. B. and Baum, H. R., "Gravity-Current Transport in Building Fires": *Transport Phenomena in Combustion - Proceedings of the Eighth International Symposium on Transport Phenomena in Combustion*, Ed. Chan, S. H., pp. 745-756.
- ¹⁶ Evans, D. D., 1995, "Ceiling Jet Flows", *The SFPE Handbook of Fire Protection Engineering*, 2nd edition, the National Fire Protection Association, Ed. DiNenno, P. J. et al, pp.2.33-2.39.
- ¹⁷ Beck, V. R., 1991, "Fire Safety System Design Using Risk Assessment Models: Developments in Australia," *Fire Safety Science - Proceedings of the Third International Symposium*, the University of Edinburgh, Scotland, pp.45-59.

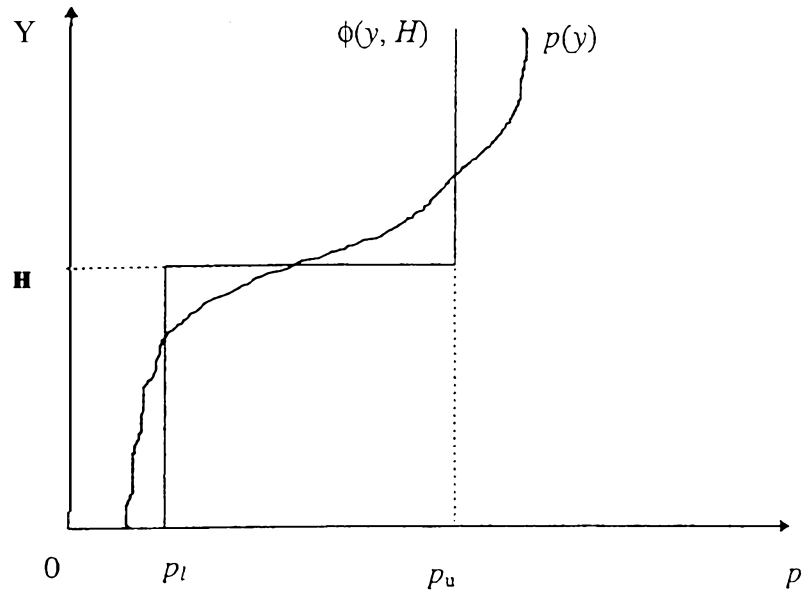
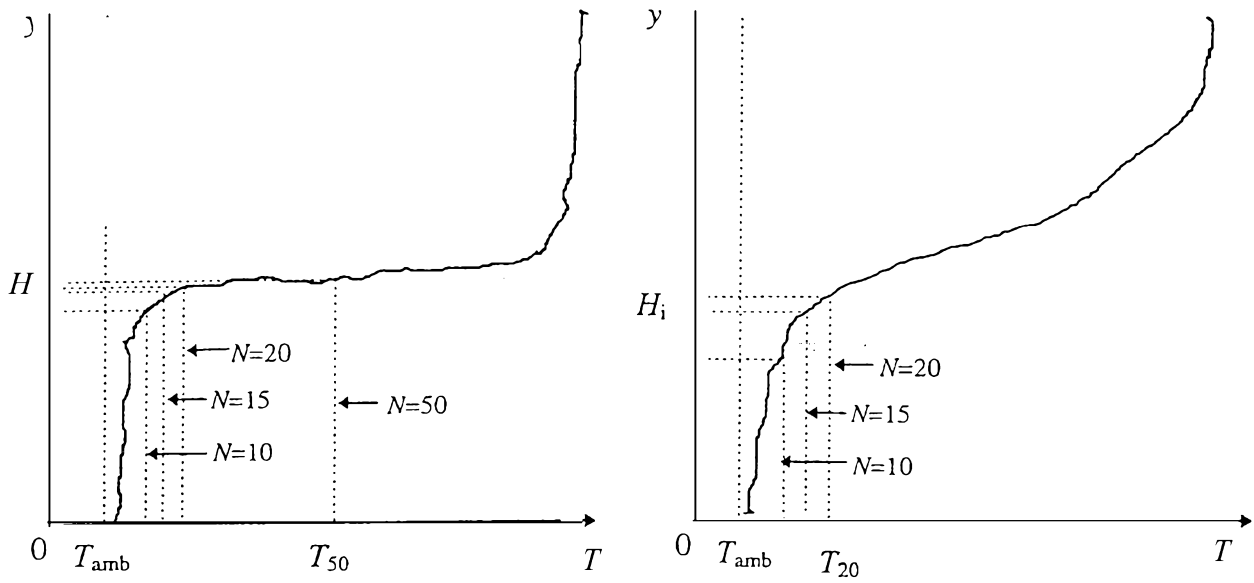


Figure 3. Parameter distribution and the $\phi(y, H)$ function.



- (a) Temperature profile with a large gradient around the interface region;
 (b) Temperature profile with a relatively small gradient around the interface region.

Figure 1. Differences in the interface heights determined with various N values

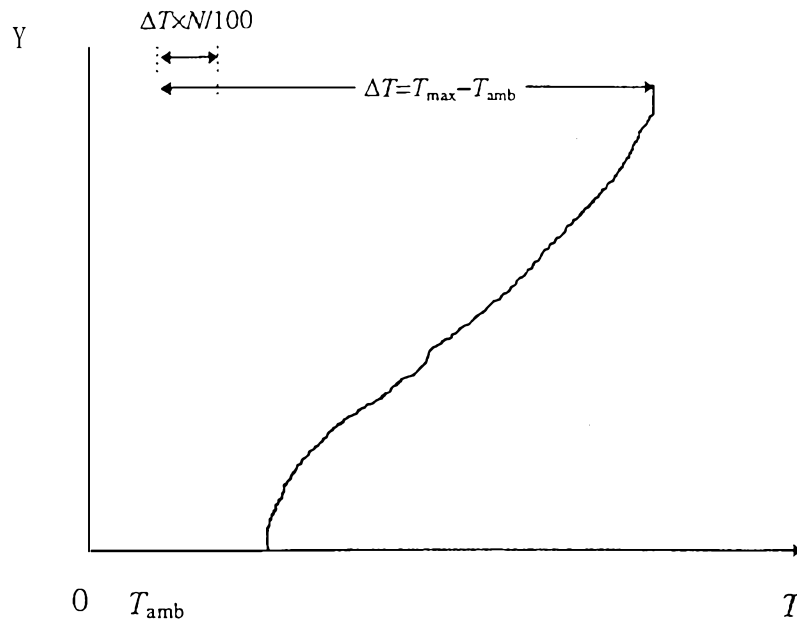


Figure 2. A case of indefinite interface according to the N-percentage rule.

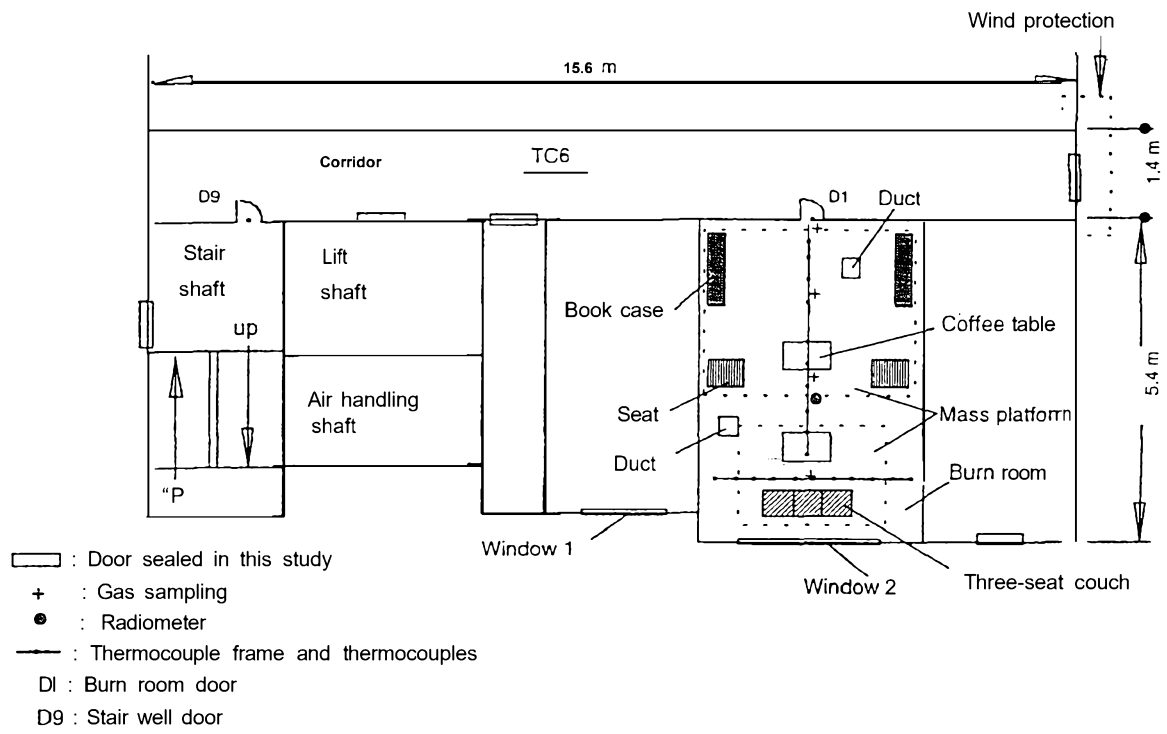
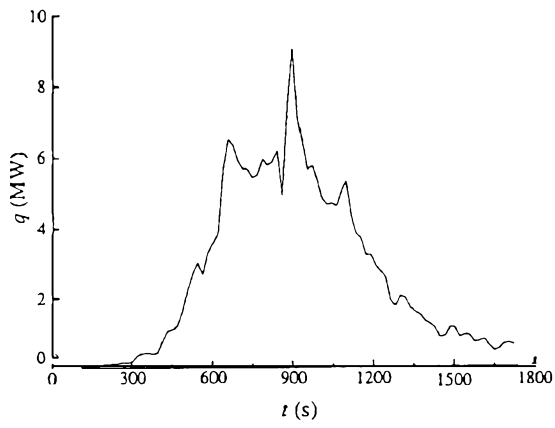
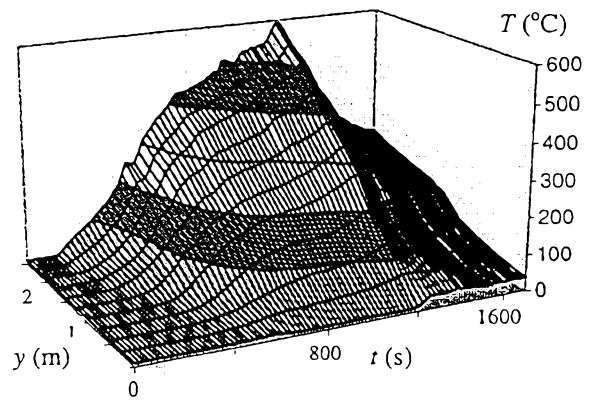


Figure 4. The first floor layout of the experimental facility and the fuel configuration in the burn room.



(a) Heat release rate in the burn room;



(b) Temperature vertical distribution in the corridor.

Figure 5. Measured results of the first experiment.

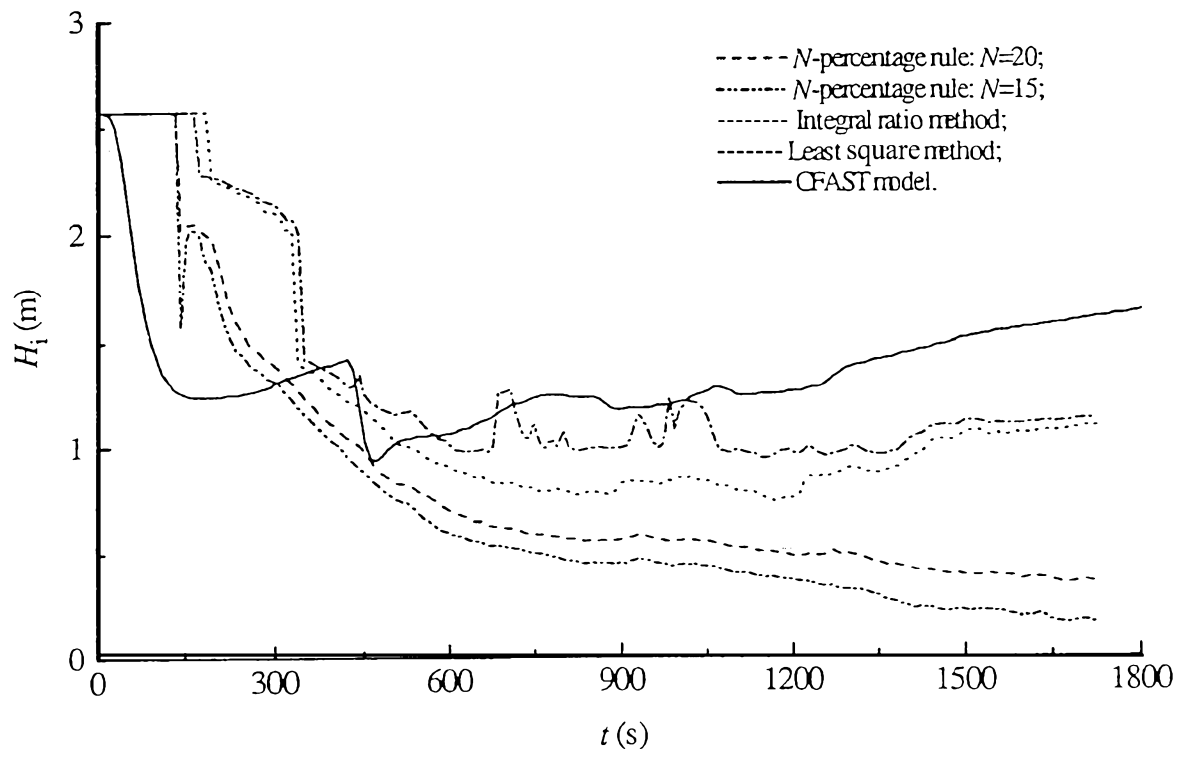


Figure 6. Interface heights determined with various methods for Case 1 experiment.

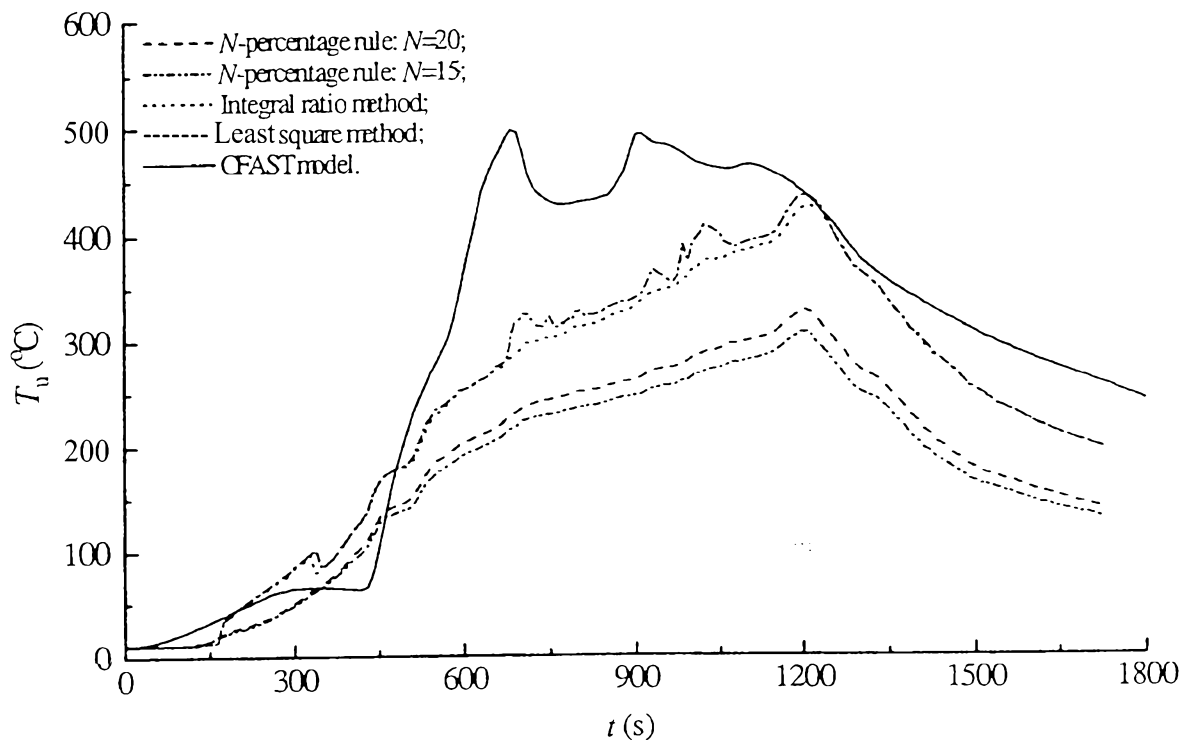


Figure 7. Average upper zone temperatures corresponding to various interface heights for Case 1 experiment.

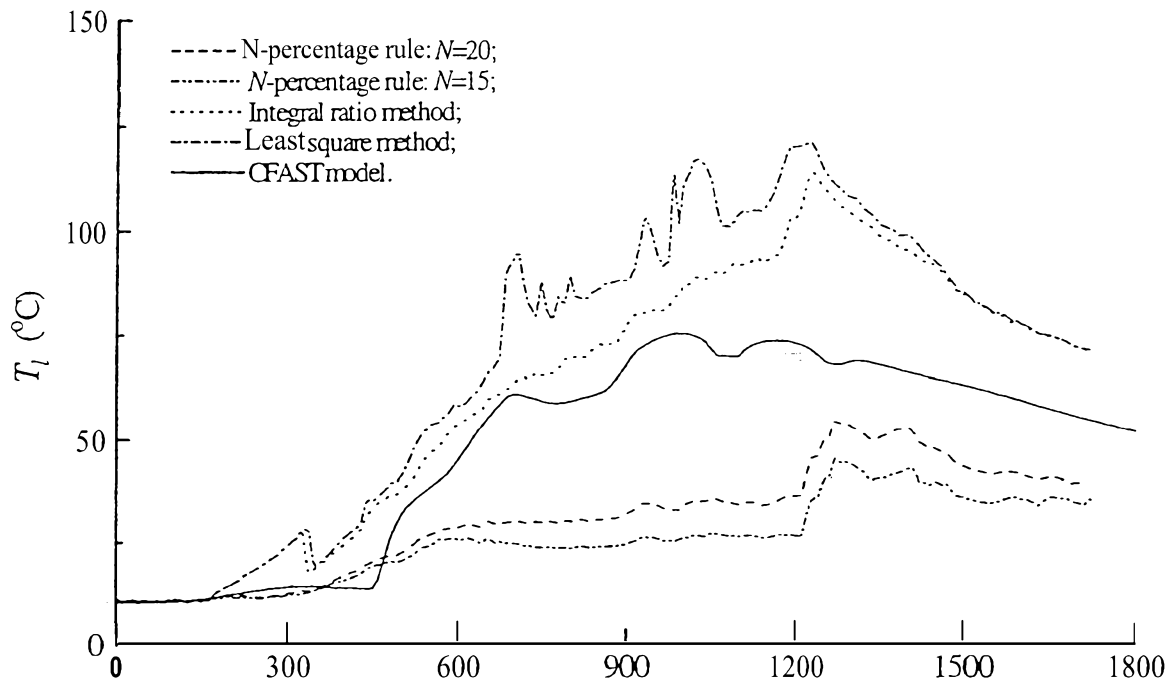
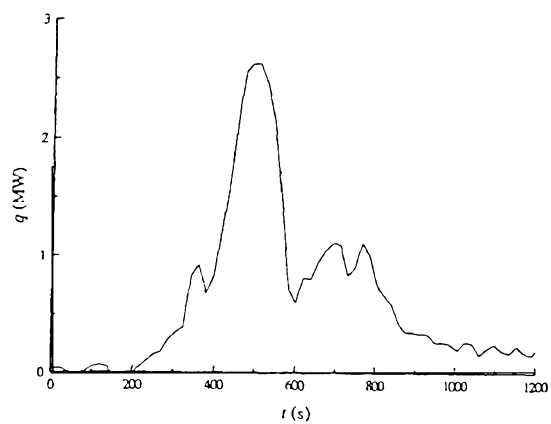
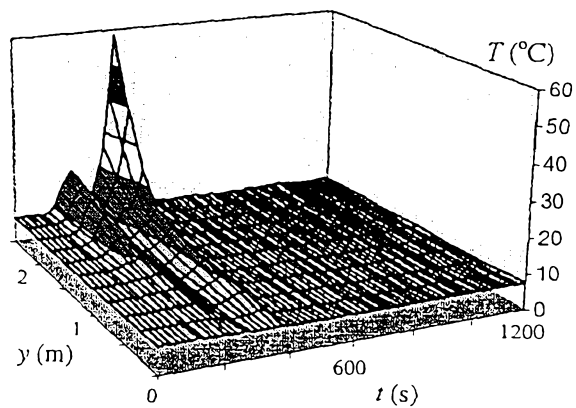


Figure 8. Average lower zone temperatures corresponding to various interface heights for Case 1 experiment.



(a) Heat release rate in the bum room;



(b) Temperature vertical distribution in the corridor.

Figure 9. Measured results of Case 2 experiment.

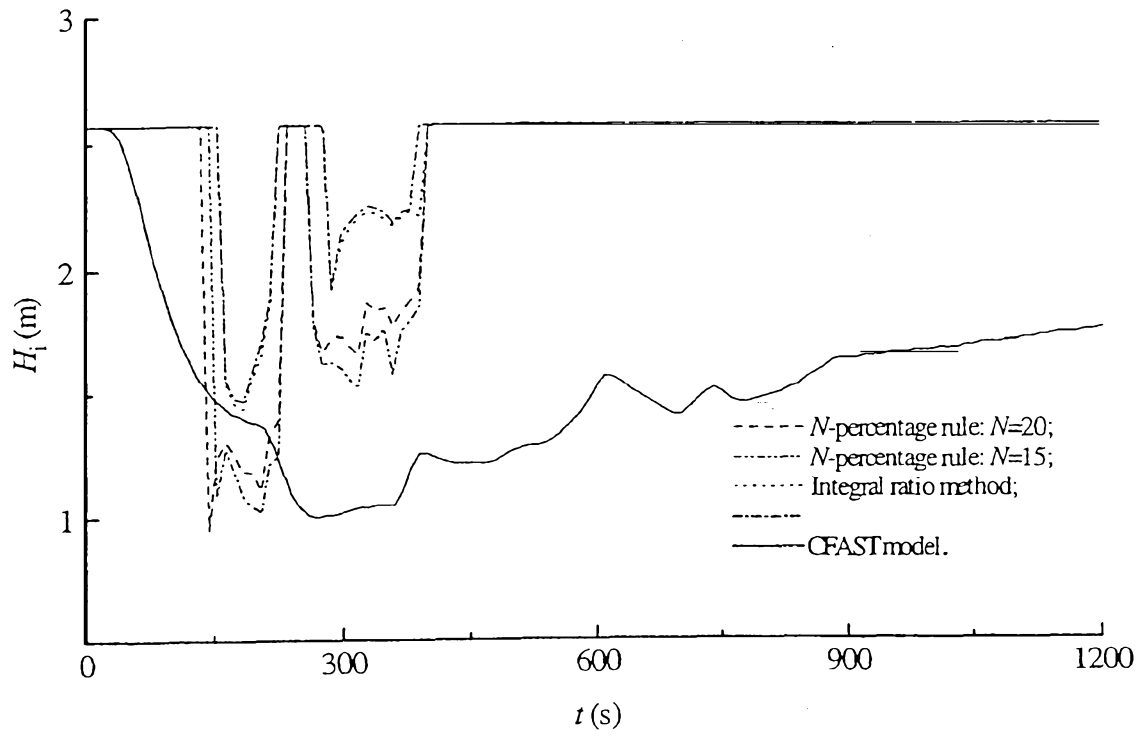


Figure 10. Interface heights determined with various methods for Case 2 experiment.

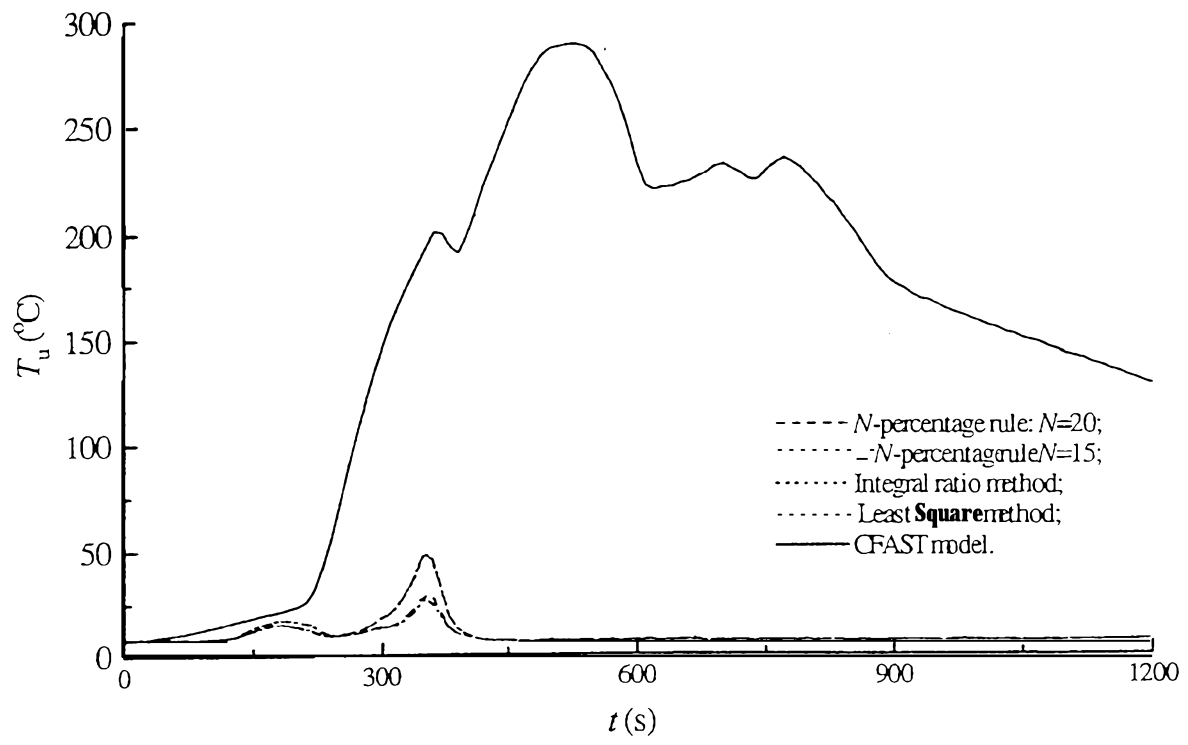


Figure 11. Average upper zone temperatures corresponding to various interface heights for Case 2 experiment.

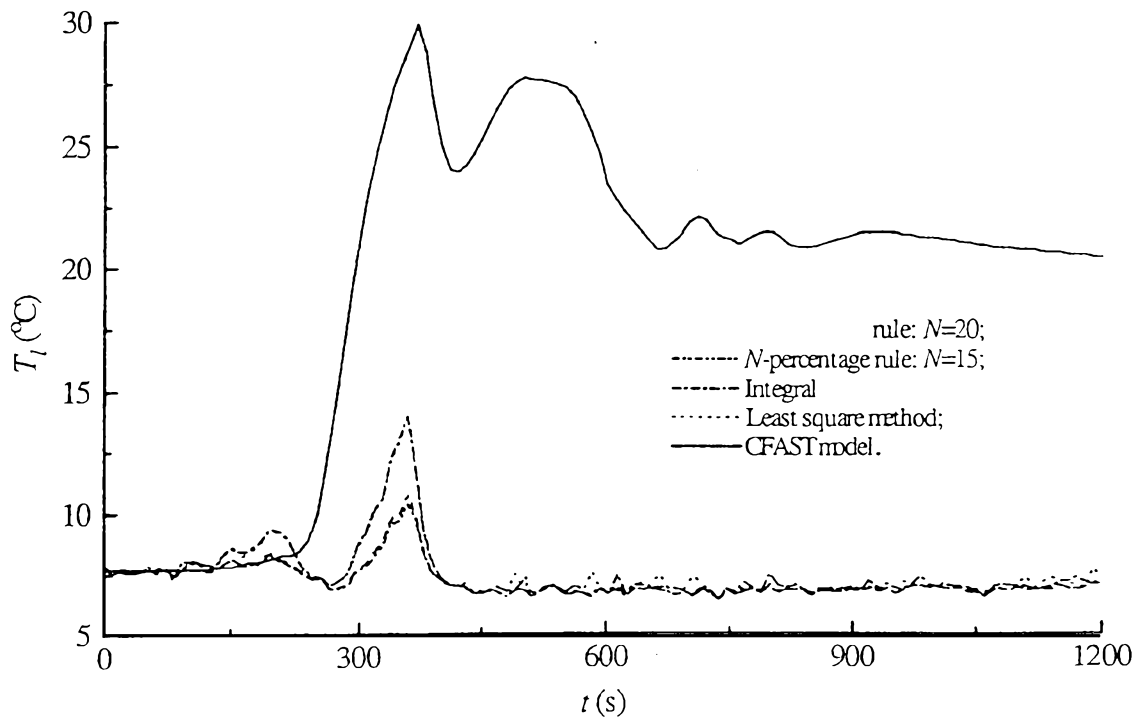


Figure 12. Average lower zone temperatures corresponding to various interface heights for Case 2 experiment.

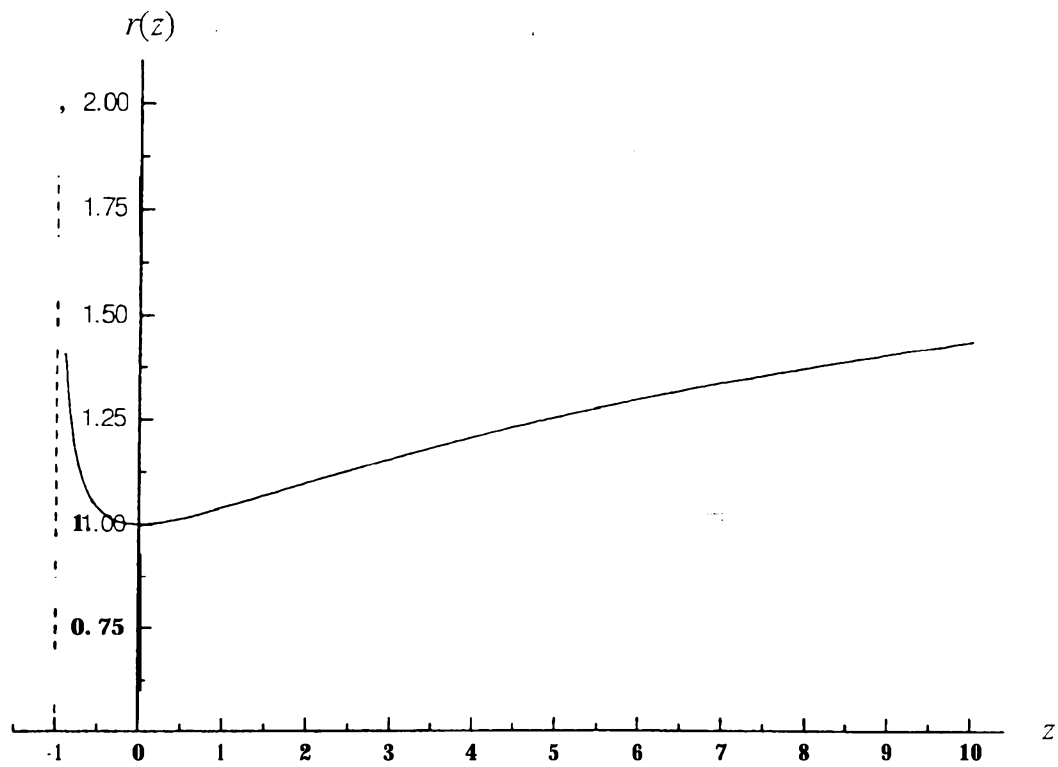


Figure 13. The graph of function $r(z) = \left(\frac{1}{2} + \frac{1}{z}\right) \log(z-1)$.